DESY 97-235
KAIST-TH 12/97
BUTP-97/34
SNUTP 97-169

DESY 97-235
KAIST-TH 12/97
BUTP-97/34
SNUTP 97-169
December 1997

Contribution of b $\to$ sgg through the QCD anomaly in exclusive decays $B^{\pm} \to (\eta', \eta)(K^{\pm}, K^{*\pm})$ and $B^0 \to (\eta', \eta)(K^0, K^{*0})$

A. Ali[a], J. Chay[b], C. Greub[c] and P. Ko[d]

[a]**Deutsches Elektronen Synchrotron DESY, Hamburg, Germany**
[b]**Department of Physics, Korea University, Seoul 136-701, Korea**
[c] **Inst. f. Theor. Physik, Univ. Bern, Bern, Switzerland**
[d] **Department of Physics, KAIST, Taejon 305-701, Korea**

Abstract

We compute the decay rates for the exclusive decays $B^{\pm} \to (\eta', \eta)(K^{\pm}, K^{*\pm})$ and $B^0 \to (\eta', \eta)(K^0, K^{*0})$ in a QCD-improved factorization framework by including the contribution from the process $b \to sgg \to s(\eta', \eta)$ through the QCD anomaly. This method provides an alternative estimate of the contribution $b \to sc\bar{c} \to s(\eta, \eta')$ to these decays as compared to the one using the intrinsic charm content of the η' and η mesons determined through the decays $J/\psi \to (\eta, \eta', \eta_c)\gamma$. The advantage of computing the relevant matrix elements via the QCD anomaly governing the transition $gg \to (\eta', \eta)$ is that there is no sign ambiguity in these contributions relative to the matrix elements from the rest of the operators in the weak effective Hamiltonian. Numerically, the QCD anomaly method and the one using the radiative decays $J/\psi \to (\eta, \eta', \eta_c)\gamma$ give similar branching ratios for the decays of interest here. The resulting branching ratios are compared with the CLEO data on $B^{\pm} \to \eta' K^{\pm}$ and $B^0 \to \eta' K^0$ and predictions are made for the rest.

(Submitted to Physics Letters B)

1. Introduction

The CLEO collaboration has recently reported measurements in a number of exclusive two-body non-leptonic decays of the type $B \to h_1 h_2$, where h_1 and h_2 are light mesons and the inclusive decay $B^\pm \to \eta' X_s$ [1] - [5]. In particular, large branching ratios into the final states including η' are reported [1, 5]:

$$B(B^\pm \to \eta' + X_s) = (6.2 \pm 1.6 \pm 1.3) \times 10^{-4} \text{ (for 2.0 GeV} \leq p_{\eta'} \leq \text{2.7 GeV)}, \quad (1)$$

$$B(B^\pm \to \eta' + K^\pm) = (6.5^{+1.5}_{-1.4} \pm 0.9) \times 10^{-5}, \quad (2)$$

$$B(B^0 \to \eta' K^0) = (4.7^{+2.7}_{-2.0} \pm 0.9) \times 10^{-5} \ . \quad (3)$$

Interestingly, no decay involving the (ηK) or $(\eta, \eta')K^*$ modes of either the charged $B^\pm$ or the neutral $B^0(\overline{B^0})$ has been observed and the corresponding limits on some of these decays can be seen in [5]. Of these, the most stringent limit is reported on the decay $B^\pm \to \eta K^\pm$, for which, at 90% C.L., one has [5]

$$B(B^\pm \to \eta K^\pm) \leq 1.4 \times 10^{-5}. \quad (4)$$

These measurements have stimulated a lot of theoretical activity [6] - [18]. We will concentrate in this paper on the exclusive two-body decays $B \to (\eta', \eta)(K, K^*)$ for both neutral and charged B mesons.

In ref.. [6], two of us (A.A. and C.G.) have studied a number of non-leptonic two-body exclusive decay modes of the $B^\pm$ and B^0 mesons in the QCD-improved effective Hamiltonian approach, involving the effective four-quark and magnetic moment operators. Since the relevant matrix elements of the type $\langle h_1 h_2 | \mathcal{O}_i | B \rangle$, where $\mathcal{O}_i$ are four-quark operators, are difficult to estimate from first principles, one often resorts to the factorization approximation [19], in which the matrix elements of interest factorize into a product of two relatively more tractable hadronic matrix elements. The resulting decay rates depend on a set of effective parameters, which have to be determined from experiments. We recall that this generalized factorization approach appears to describe the two-body non-leptonic B decays involving the so-called heavy to heavy transitions reasonably well [20]. Likewise, data on $B \to K\pi$ and $B \to \pi\pi$ decays are well accounted for in this framework [6].

In contrast to the decays $B \to K\pi$ and $B \to \pi\pi$, the decays $B \to (\eta, \eta')(K, K^*)$ in the factorization approach require additionally the knowledge of the matrix elements $\langle \eta' | \overline{c} \gamma_\mu \gamma_5 c | 0 \rangle$ and $\langle \eta | \overline{c} \gamma_\mu \gamma_5 c | 0 \rangle$, emerging from the decay $b \to s(\bar{c}c) \to s(\eta', \eta)$. Parameterizing them as $\langle \eta' | \overline{c} \gamma_\mu \gamma_5 c | 0 \rangle = -i f^c_{\eta'} q_\mu$ and $\langle \eta | \overline{c} \gamma_\mu \gamma_5 c | 0 \rangle = -i f^c_\eta q_\mu$, the quantities of interest for this contribution are $f^c_{\eta'}$ and f^c_η, which are often referred to as the charm content of the η' and η, respectively [21]. These quantities are *a priori* unknown but they can be determined in a number of ways, also including the B-decays being discussed here. In [6], these quantities were determined from the decays $J/\psi \to (\eta, \eta', \eta_c)\gamma$, extending the usual (η, η')-mixing formalism [22] to the (η_c, η', η) system. Using the measured decay widths for the decays $J/\psi \to (\eta, \eta', \eta_c)\gamma$ and $(\eta_c, \eta', \eta) \to \gamma\gamma$ yields $|f^c_{\eta'}| \simeq 5.8$ MeV and $|f^c_\eta| \simeq 2.3$ MeV [6].

In the meanwhile, theoretical arguments based on $SU(3)$-breaking effects in the pseudoscalar nonet (π, K, η, η') in the chiral perturbation theory approach [23], and phenomenological analysis involving in particular the $\eta\gamma$ and $\eta'\gamma$ transition form factors [24], have put to question the conventional (one mixing-angle) octet-singlet mixing scheme for the (η, η') system. The modified two-angle mixing scheme, proposed in [23], has also implications for B decays involving

the η and η' meson in the final state. In particular, estimates of $|f^c_{\eta'}|$ and $|f^c_\eta|$ are expected to get revised. Numerically, these quantities depend on the input values of the pseudoscalar coupling constants, f_0 and f_8, and the two mixing angles, called θ_0 and θ_8. However, it is found that using the best-fit values of the parameters from [24], which are consistent with Leutwyler's estimates of the same [23], the estimate of $|f^c_{\eta'}|$ in the modified mixing scheme remains practically unaltered. In contrast, the quantity $|f^c_\eta|$ is considerably reduced due to the small value of the mixing angle in the singlet sector, which makes η an almost octet state. One finds now $|f^c_\eta| \simeq 0.9$ MeV [6]. With these estimates, it has been argued in [6] that the charm-induced contribution $b \to s(c\bar{c}) \to s(\eta', \eta)$ does not dominate the matrix element for $B^\pm \to \eta' K^\pm$. The resulting branching ratio $BR(B^\pm \to \eta' K^\pm) = (2-4) \times 10^{-5}$ is somewhat lower than but not inconsistent with the experimental number in Eq. (2).

The branching ratio for $B^\pm \to \eta' K^\pm$ (and other related decay modes) depends on the sign of the quantity $f^c_{\eta'}$ (and f^c_η involving the η meson), as well as on the phenomenological parameter ξ, which in turn determines the effective Wilson coefficients in the factorization approach [6]. It is not unreasonable to expect that the value of ξ will be similar in the decays $B \to h_1 h_2$, as the energy released in these decays are comparable; hence this parameter can be determined in a number of B decays [25]. A consistent determination of the parameter ξ will also check the consistency of the underlying theoretical framework, namely QCD-improved factorization. However, it is desirable to get independent estimates of the quantities $f^c_{\eta'}$ and f^c_η, and also settle the sign ambiguity present in the method used in [6]. We note that a recent phenomenological study has put a bound on $f^c_{\eta'}$, namely -65 MeV $\le f^c_{\eta'} \le 15$ MeV, with f^c_η being consistent with zero [24] by analyzing the Q^2 evolution of the $\eta\gamma$ and $\eta'\gamma$ form factors, respectively. The bounds on $f^c_{\eta'}$ from this method are not very stringent and the estimates of this quantity in [6] are well within these bounds.

In this letter we propose another method for computing the contribution of the amplitudes $b \to s(gg) \to s(\eta', \eta)$. This method is based on calculating the amplitude for the chromomagnetic penguin process $b \to sgg$, followed by the transitions $gg \to (\eta', \eta)$ which are calculated using the QCD anomaly, determining both the sign and magnitude of these contributions. As discussed below, the numerical values of $f^c_{\eta'}$ and f^c_η now depend on the charm quark mass (both of them being essentially proportional to m_c^{-2}). Varying m_c in the range 1.3 - 1.5 GeV, we find that the QCD-anomaly-method gives $f^c_{\eta'} = -3.1$ (-2.3) MeV and $f^c_\eta = -1.2$ (-0.9) MeV. Hence, in absolute value, f^c_η turns out to be very close to the one obtained in the (η_c, η', η)-mixing formalism [6] (the two estimates almost coincide for $m_c = 1.5$ GeV), but the value of $f^c_{\eta'}$ is typically a factor 2 smaller in the QCD-anomaly method. The branching ratios for $B^\pm \to (\eta', \eta)(K^\pm, K^{*\pm})$ and $B^0 \to (\eta', \eta)(K^0, K^{*0})$ based on the QCD-anomaly method are calculated in this letter and compared with the present CLEO measurements and with the ones in [6]. We find that the theoretical branching ratios for $B^\pm \to \eta' K^\pm$ and $B^0 \to \eta' K^0$ are almost equal and both are in the range $(2-4) \times 10^{-5}$, in agreement with the estimates in [6].

2. Estimate of b $\to (\eta, \eta')$s via QCD anomaly

We write the effective Hamiltonian $H_{\rm eff}$ for the $\Delta B = 1$ hadronic transitions as

$$H_{\rm eff} = \frac{G_F}{\sqrt{2}} \left[V_{ub} V^*_{uq} \left(C_1 O^u_1 + C_2 O^u_2 \right) + V_{cb} V^*_{cq} \left(C_1 O^c_1 + C_2 O^c_2 \right) - V_{tb} V^*_{tq} \left(\sum_{i=3}^{10} C_i \, O_i + C_g O_g \right) \right] \quad , \tag{5}$$

where $q = d, s$. The operators read

$$\begin{aligned}
O_1^u &= (\bar{u}_\alpha b_\alpha)_{V-A}\,(\bar{q}_\beta u_\beta)_{V-A} \qquad O_1^c = (\bar{c}_\alpha b_\alpha)_{V-A}\,(\bar{q}_\beta c_\beta)_{V-A} \\
O_2^u &= (\bar{u}_\beta b_\alpha)_{V-A}\,(\bar{q}_\alpha u_\beta)_{V-A} \qquad O_2^c = (\bar{c}_\beta b_\alpha)_{V-A}\,(\bar{q}_\alpha c_\beta)_{V-A} \\
O_3 &= (\bar{q}_\alpha b_\alpha)_{V-A}\sum_{q'}\left(\bar{q}'_\beta q'_\beta\right)_{V-A} \qquad O_4 = (\bar{q}_\beta b_\alpha)_{V-A}\sum_{q'}\left(\bar{q}'_\alpha q'_\beta\right)_{V-A} \\
O_5 &= (\bar{q}_\alpha b_\alpha)_{V-A}\sum_{q'}\left(\bar{q}'_\beta q'_\beta\right)_{V+A} \qquad O_6 = (\bar{q}_\beta b_\alpha)_{V-A}\sum_{q'}\left(\bar{q}'_\alpha q'_\beta\right)_{V+A} \\
O_7 &= \frac{3}{2}(\bar{q}_\alpha b_\alpha)_{V-A}\sum_{q'} e_{q'}\left(\bar{q}'_\beta q'_\beta\right)_{V+A} \qquad O_8 = \frac{3}{2}(\bar{q}_\beta b_\alpha)_{V-A}\sum_{q'} e_{q'}\left(\bar{q}'_\alpha q'_\beta\right)_{V+A} \\
O_9 &= \frac{3}{2}(\bar{q}_\alpha b_\alpha)_{V-A}\sum_{q'} e_{q'}\left(\bar{q}'_\beta q'_\beta\right)_{V-A} \qquad O_{10} = \frac{3}{2}(\bar{q}_\beta b_\alpha)_{V-A}\sum_{q'} e_{q'}\left(\bar{q}'_\alpha q'_\beta\right)_{V-A} \\
O_g &= (g_s/8\pi^2)\, m_b\, \bar{s}_\alpha\, \sigma^{\mu\nu}\,(1+\gamma_5)\,(\lambda^A_{\alpha\beta}/2)\, b_\beta\; G^A_{\mu\nu} \quad . \qquad (6)
\end{aligned}$$

Here α and β are the $SU(3)$ color indices and $\lambda^A_{\alpha\beta}, A = 1, ..., 8$, are the Gell-Mann matrices. The subscripts $V \pm A$ represent the chiral projections $1 \pm \gamma_5$. $G^A_{\mu\nu}$ denotes the gluonic field strength tensor. The operators O_1 and O_2 are the current-current operators, $O_3, ..., O_6$ the so-called gluonic penguin operators and $O_7, ..., O_{10}$ are the electroweak penguin operators. Finally, O_g is the gluonic dipole operator. In the following we use the next-to-leading logarithmic values (NLL) (with respect to QCD) for $C_1, ..., C_6$, computed in [26], while the remaining coefficients are taken at leading logarithmic precision (LL). Taking $\alpha_s(m_Z) = 0.118$, $\alpha_{ew}(m_Z) = 1/128$ and $m_{top}^{pole} = 175$ GeV, the coefficients in the naive dimensional renormalization scheme (NDR) (evaluated at the renormalization scale $\mu = 2.5$ GeV) read: $C_1 = 1.117$, $C_2 = -0.257$, $C_3 = 0.017$, $C_4 = -0.044$, $C_5 = 0.011$, $C_6 = -0.056$, $C_7 = -1 \times 10^{-5}$, $C_8 = 5 \times 10^{-4}$, $C_9 = -0.010$, $C_{10} = 0.002$ and $C_g = -0.158$. Among the coefficients of the electroweak penguins only C_9 has a sizable coefficient, which arises mainly from the Z^0 penguin.

Working consistently to the precision mentioned above, we include one-loop QCD corrections to the partonic matrix elements of the operators $O_1, ..., O_6$ and the tree-level diagram associated with O_g, where the gluon splits into a quark-antiquark pair. These issues are discussed in detail in ref. [6]. In addition, we include the photonic penguin diagram associated with the current-current operators O_1 and O_2. All these corrections can be absorbed into effective Wilson coefficients $C_i^{\rm eff}$ $(i = 1, ..., 10)$ multiplying the four-Fermi operators $O_1, ..., O_{10}$ in the basis (6). While $C_1^{\rm eff}, ..., C_6^{\rm eff}$ are given in Eq. (2.5) in ref. [6], the remaining effective coefficients read

$$C_7^{\rm eff} = C_7 + \frac{\alpha_{ew}}{8\pi} C_e \quad , C_8^{\rm eff} = C_8 \quad , C_9^{\rm eff} = C_9 + \frac{\alpha_{ew}}{8\pi} C_e \quad , C_{10}^{\rm eff} = C_{10} \quad , \qquad (7)$$

where

$$C_e = -\frac{8}{9}(3C_2 + C_1) \sum_{q'=u,c} \frac{V_{q'b} V^*_{q'q}}{V_{tb} V^*_{tq}} \left(\frac{2}{3} + \frac{2}{3} \log \frac{m_{q'}^2}{\mu^2} - \Delta F_1 \left(\frac{k^2}{m_{q'}^2} \right) \right) \quad . \qquad (8)$$

The function ΔF_1 is also given in ref. [6]. In the following, we often use the following linear combinations of effective Wilson coefficients ($N_c = 3$ is the number of colors):

$$a_i = C_i^{\rm eff} + \frac{1}{N_c} C_{i+1}^{\rm eff} \quad (i = \text{odd}) \quad ; \; a_i = C_i^{\rm eff} + \frac{1}{N_c} C_{i-1}^{\rm eff} \quad (i = \text{even}) \quad . \qquad (9)$$

As described in detail in ref. [6], the hadronic matrix elements $\langle h_1 h_2|C_i^{\rm eff}O_i|B\rangle$ for the two-body decays of the form $B \to h_1 h_2$ are now readily decomposed into various form factors and decay constants when applying the factorization approximation. If $\eta^{(\prime)}$ is involved in the final state, the factorization of O_1^c and O_2^c brings in the matrix elements

$$\langle \eta^{(\prime)}|\bar{c}\gamma_\mu\gamma_5 c|0\rangle \tag{10}$$

which have to be estimated. We model them by annihilating the charm-anticharm pair into two gluons, followed by the transition $gg \to \eta^{(\prime)}$ (see Fig. 1). The first part of this two-step process, i.e. $b \to s(\bar{c}c \to g(k_1)g(k_2))$ which amounts to calculating the charm-quark-loop from which two gluons are emitted, has been worked out by Simma and Wyler [27] in the context of a calculation in the full theory. Their result is readily translated to our effective theory approach and can be compactly written as a new (induced) effective Hamiltonian $H_{\rm eff}^{gg}$,

$$H_{\rm eff}^{gg} = -\frac{\alpha_s}{2\pi}\left(C_2^{\rm eff} + \frac{C_1^{\rm eff}}{N_c}\right)\frac{G_F}{\sqrt{2}}V_{cb}V_{cs}^*\Delta i_5(\frac{q^2}{m_c^2})\frac{1}{k_1\cdot k_2}G_a^{\alpha\beta}(D_\beta\tilde{G}_{\alpha\mu})_a\,\overline{s}\gamma^\mu(1-\gamma_5)b \quad , \tag{11}$$

with $\tilde{G}_{\mu\nu} = \frac{1}{2}\epsilon_{\mu\nu\alpha\beta}G^{\alpha\beta}$ ($\epsilon_{0123} = +1$). In this formula, which holds for on-shell gluons ($q^2 = (k_1+k_2)^2 = 2k_1\cdot k_2$), the sum over color indices is understood. The function $\Delta i_5(q^2/m_c^2)$ is defined as

$$\Delta i_5(z) = -1 + \frac{1}{z}\Big[\pi - 2\arctan(\frac{4}{z}-1)^{1/2}\Big]^2, \text{ for } 0 < z < 4 \quad . \tag{12}$$

Note that the $b \to sgg$ calculation brings in an explicit factor of α_s. However, as shown below, this explicit α_s factor gets absorbed into the matrix element of the operator resulting from the anomaly. So, to the order that we are working, we use the coefficients $C_1^{\rm eff}$ and $C_2^{\rm eff}$ in eq. (11). By expanding the function $\Delta i_5(q^2/m_c^2)$ in inverse powers of m_c^2, it is easy to see that the leading $(1/m_c^2)$ term in Eq. (11) generates the chromomagnetic analogue of the operator considered by Voloshin [28] to calculate the power $(1/m_c^2)$ correction in the radiative decay $B \to X_s\gamma$. It should be remarked that the corresponding $u\bar{u}$ contribution in Fig. 1 is suppressed due to the unfavourable CKM factors. The $t\bar{t}$ contribution is included in the effective Hamiltonian via the $bsgg$ piece present in the operator O_g. However, in the factorization framework, the $bsgg$ term in O_g does not contribute to the decays discussed. So, the $c\bar{c}$ contribution in Fig. 1 is the only one that survives.

The (factorizable) contribution from Eq. (11) in the decays $B \to (\eta,\eta')(K,K^*)$ is of the same order (in α_s) as those of the other operators taken into account in [6]. It should be remarked that in calculating the amplitude $b \to sgg$, there are more contributions in this order in α_s than what is shown in Eq. (11) and Fig. 1. However, the diagrams where one of the gluons is present in the final state yielding $b \to sg(\eta,\eta')$ are not expected to contribute significantly to the exclusive two-body decays, but rather induce multibody decays. Certainly, these configurations have to be included in inclusive decays $B \to (\eta,\eta')X_s$ [7] but can be neglected in the exclusive decays $B \to (\eta,\eta')(K,K^*)$. Likewise, configurations in which one of the gluons emanates from the effective bsg vertex and the other is bremsstrahled from the b or s-quark (or from the spectator anti-quark in the B meson) to form an η' or η are non-factorizing contributions and they are ignored as the rest of the amplitudes are also calculated in the factorization approximation.

Working out the hadronic matrix element of Eq. (11) using factorization, we now need to evaluate the matrix elements

$$\langle \eta^{(\prime)}|G_a^{\alpha\beta}(D_\beta\tilde{G}_{\alpha\mu,a})|0\rangle \quad . \tag{13}$$

The operator in Eq. (13) can be written as

$$G_a^{\alpha\beta}(D_\beta \tilde{G}_{\alpha\mu})_a = \partial_\beta(G_a^{\alpha\beta}\tilde{G}_{\alpha\mu,a}) - (D_\beta G^{\alpha\beta})_a \tilde{G}_{\alpha\mu,a} \quad . \tag{14}$$

We can discard the second term since it is suppressed by an additional power of g_s which follows on using the equation of motion, and furthermore, the first term is enhanced by N_c in the large N_c limit. The matrix elements of $\partial_\beta(G_a^{\alpha\beta}\tilde{G}_{\alpha\mu,a})$ are related to those of $G\tilde{G}$; more explicitly

$$\partial_\beta \langle \eta^{(\prime)}|G_a^{\alpha\beta}\tilde{G}_{\alpha\mu,a}|0\rangle = \frac{iq_\mu}{4}\langle \eta^{(\prime)}|G_a^{\alpha\beta}\tilde{G}_{\alpha\beta,a}|0\rangle \quad . \tag{15}$$

The conversion of the gluons into η and η' is described by an amplitude which is fixed by the $SU(3)$ symmetry and the axial $U(1)$ current triangle anomaly. The matrix elements for $G\tilde{G}$ can be written as [29]

$$\langle \eta^{(\prime)}|\frac{\alpha_s}{4\pi}G_a^{\alpha\beta}\tilde{G}_{\alpha\beta,a}|0\rangle = m^2_{\eta^{(\prime)}} f^u_{\eta^{(\prime)}} \quad . \tag{16}$$

In Eqs. (16) the decay constants $f^u_{\eta'}$ and f^u_η read

$$f^u_\eta = \frac{f_8}{\sqrt{6}}\cos\theta_8 - \frac{f_0}{\sqrt{3}}\sin\theta_0 \quad , \quad f^u_{\eta'} = \frac{f_8}{\sqrt{6}}\sin\theta_8 + \frac{f_0}{\sqrt{3}}\cos\theta_0 \quad , \tag{17}$$

where the coupling constants f_8, f_0 and the mixing angles θ_8 and θ_0 have been introduced earlier. We follow here the two-angle (η, η') mixing formalism of ref. [23], where the mass eigenstates $|\eta\rangle$ and $|\eta'\rangle$ have the following decompositions:

$$\begin{aligned} |\eta\rangle &= \cos\theta_8|\eta_8\rangle - \sin\theta_0|\eta_0\rangle, \\ |\eta'\rangle &= \sin\theta_8|\eta_8\rangle + \cos\theta_0|\eta_0\rangle. \end{aligned} \tag{18}$$

Collecting the individual steps, the matrix elements in Eqs. (13) can be written as

$$\langle \eta^{(\prime)}(q)|\frac{\alpha_s}{4\pi}G_a^{\alpha\beta}(D_\beta \tilde{G}_{\alpha\mu a})|0\rangle = iq_\mu \frac{m^2_{\eta^{(\prime)}}}{4} f^u_{\eta^{(\prime)}} \quad . \tag{19}$$

One would have naively expected that the gluonic matrix elements are small since they contain an extra factor of α_s. However, as shown by Eqs. (19), this is obviously not the case and the gluon operator with α_s as a whole is responsible for the invariant mass of the $\eta^{(\prime)}$ mesons. Also, the combination entering in Eqs. (19) involving the product of α_s and the gluon field operators is independent of the renormalization scale.

3. Matrix elements for the decays $\mathbf{B^\pm \to (\eta', \eta)(K^\pm, K^{*\pm})}$ and $\mathbf{B^0 \to (\eta', \eta)(K, K^{*0})}$

To compute the complete amplitude for the exclusive decays, one has to combine the contribution from the decay $b \to s(c\bar{c}) \to s(gg) \to s\eta^{(\prime)}$ discussed in the previous section with all the others arising from the four-quark and chromomagnetic operators, as detailed in [6]. The resulting amplitudes in the factorization approximation are listed below for all the eight cases of interest $B^\pm \to (\eta', \eta)(K^\pm, K^{*\pm})$ and $B^0 \to (\eta', \eta)(K^0, K^{*0})$. The expressions are given for the decays of the B^- and $\overline{B^0}$ mesons; the ones for the charge conjugate decays are obtained by complex conjugating the CKM factors.

(i) $\mathbf{B^- \to K^- \eta^{(\prime)}}$

$$
\begin{aligned}
M &= \frac{G_F}{\sqrt{2}} \Bigg\{ V_{ub}V_{us}^* \left[a_2 + a_1 \frac{m_B^2 - m_{\eta^{(\prime)}}^2}{m_B^2 - m_K^2} \frac{F_0^{B\to\eta^{(\prime)}}(m_K^2)}{F_0^{B\to K^-}(m_{\eta^{(\prime)}}^2)} \frac{f_K}{f_{\eta^{(\prime)}}^u} \right] - V_{cb}V_{cs}^*\, a_2 \Delta i_5\Big(\frac{m_{\eta^{(\prime)}}^2}{m_c^2}\Big) \\
&\quad - V_{tb}V_{ts}^* \Bigg[2(a_3 - a_5) + \frac{1}{2}(a_9 - a_7) + \Bigg(a_3 - a_5 - \frac{1}{2}(a_9 - a_7) + a_4 - \frac{1}{2}a_{10} \\
&\quad + (a_6 - \frac{1}{2}a_8) \frac{m_{\eta^{(\prime)}}^2}{m_s(m_b - m_s)} \Bigg) \frac{f_{\eta^{(\prime)}}^s}{f_{\eta^{(\prime)}}^u} - (a_6 - \frac{1}{2}a_8) \frac{m_{\eta^{(\prime)}}^2}{m_s(m_b - m_s)} \\
&\quad + \left(a_4 + a_{10} + \frac{2(a_6 + a_8)m_K^2}{(m_s + m_u)\,(m_b - m_u)} \right) \frac{m_B^2 - m_{\eta^{(\prime)}}^2}{m_B^2 - m_K^2} \frac{F_0^{B\to\eta^{(\prime)}}(m_K^2)}{F_0^{B\to K^-}(m_{\eta^{(\prime)}}^2)} \frac{f_K}{f_{\eta^{(\prime)}}^u} \Bigg] \Bigg\} \\
&\times \langle K^-|\bar{s}\, b_-|B^-\rangle \, \langle \eta^{(\prime)}|\bar{u}\, u_-|0\rangle
\end{aligned}
\tag{20}
$$

where

$$
\langle K^-|\bar{s}\, b_-|B^-\rangle \, \langle \eta^{(\prime)}|\bar{u}\, u_-|0\rangle = i\, f_{\eta^{(\prime)}}^u \, (m_B^2 - m_K^2)\, F_0^{B\to K^-}(m_{\eta^{(\prime)}}^2). \tag{21}
$$

The coefficients a_i are defined in Eq. (9) and the short-hand notation $\bar{u}\, u_-$ stands for $\bar{u}\, u_- = \bar{u}\gamma_\mu(1-\gamma_5)u$. The quantities f_η^u and $f_{\eta'}^u$ are given in Eqs. (17), while f_η^s and $f_{\eta'}^s$ read

$$
f_{\eta'}^s = -2\,\frac{f_8}{\sqrt{6}}\,\sin\theta_8 + \frac{f_0}{\sqrt{3}}\,\cos\theta_0 \quad , \quad f_\eta^s = -2\,\frac{f_8}{\sqrt{6}}\,\cos\theta_8 - \frac{f_0}{\sqrt{3}}\,\sin\theta_0 \quad . \tag{22}
$$

Note that the matrix elements of the pseudoscalar density have been expressed as

$$
\langle \eta^{(\prime)}|\bar{s}\gamma_5 s|0\rangle = i\frac{m_{\eta^{(\prime)}}^2}{2m_s}(f_{\eta^{(\prime)}}^u - f_{\eta^{(\prime)}}^s). \tag{23}
$$

(ii) $\mathbf{B^- \to K^{*-} \eta^{(\prime)}}$

$$
\begin{aligned}
M &= \frac{G_F}{\sqrt{2}} \Bigg\{ V_{ub}V_{us}^* \left[a_2 + a_1 \frac{F_1^{B\to\eta^{(\prime)}}(m_{K^*}^2)}{A_0^{B\to K^*}(m_{\eta^{(\prime)}}^2)} \frac{f_{K^*}}{f_{\eta^{(\prime)}}^u} \right] - V_{cb}V_{cs}^*\, a_2\, \Delta i_5\Big(\frac{m_{\eta^{(\prime)}}^2}{m_c^2}\Big) \\
&\quad - V_{tb}V_{ts}^* \Bigg[2(a_3 - a_5) + \frac{1}{2}(a_9 - a_7) + \Bigg(a_3 - a_5 - \frac{1}{2}(a_9 - a_7) + a_4 - \frac{1}{2}a_{10} \\
&\quad - (a_6 - \frac{1}{2}a_8) \frac{m_{\eta^{(\prime)}}^2}{m_s(m_b + m_s)} \Bigg) \frac{f_{\eta^{(\prime)}}^s}{f_{\eta^{(\prime)}}^u} + (a_6 - \frac{1}{2}a_8) \frac{m_{\eta^{(\prime)}}^2}{m_s(m_b + m_s)} \\
&\quad + (a_4 + a_{10}) \frac{F_1^{B\to\eta^{(\prime)}}(m_{K^*}^2)}{A_0^{B\to K^*}(m_{\eta^{(\prime)}}^2)} \frac{f_{K^*}}{f_{\eta^{(\prime)}}^u} \Bigg] \Bigg\} \, \langle K^{*-}|\bar{s}\, b_-|B^-\rangle \, \langle \eta^{(\prime)}|\bar{u}\, u_-|0\rangle
\end{aligned}
\tag{24}
$$

with

$$
\langle K^{*-}|\bar{s}\, b_-|B^-\rangle \, \langle \eta^{(\prime)}|\bar{u}\, u_-|0\rangle = -i\, f_{\eta^{(\prime)}}^u \, 2m_{K^*}\, (p_B \epsilon_{K^*}^*)\, A_0^{B\to K^*}(m_{\eta^{(\prime)}}^2). \tag{25}
$$

(iii) $\overline{\mathbf{B^0}} \to \overline{\mathbf{K^0}}\eta^{(\prime)}$

$$
\begin{aligned}
M &= \frac{G_F}{\sqrt{2}}\Big\{V_{ub}V_{us}^* a_2 - V_{cb}V_{cs}^* a_2 \Delta i_5\big(\frac{m^2_{\eta^{(\prime)}}}{m_c^2}\big) \\
&- V_{tb}V_{ts}^*\Big[2(a_3-a_5)+\frac{1}{2}(a_9-a_7)+\Big(a_3-a_5-\frac{1}{2}(a_9-a_7)+a_4-\frac{1}{2}a_{10} \\
&\quad +(a_6-\frac{1}{2}a_8)\frac{m^2_{\eta^{(\prime)}}}{m_s(m_b-m_s)}\Big)\frac{f^s_{\eta^{(\prime)}}}{f^u_{\eta^{(\prime)}}} - (a_6-\frac{1}{2}a_8)\frac{m^2_{\eta^{(\prime)}}}{m_s(m_b-m_s)} \\
&+ \Big(a_4-\frac{1}{2}a_{10}+\frac{(2a_6-a_8)m_K^2}{(m_s+m_d)(m_b-m_d)}\Big)\frac{m_B^2-m^2_{\eta^{(\prime)}}}{m_B^2-m_K^2}\frac{F_0^{B\to\eta^{(\prime)}}(m_K^2)}{F_0^{B\to K}(m^2_{\eta^{(\prime)}})}\frac{f_{K_0}}{f^u_{\eta^{(\prime)}}}\Big]\Big\} \\
&\times \langle\overline{K^0}|\overline{s}b_-|\overline{B^0}\rangle\langle\eta^{(\prime)}|\overline{u}u_-|0\rangle. \qquad (26)
\end{aligned}
$$

(iv) $\overline{\mathbf{B^0}} \to \overline{\mathbf{K^{*0}}}\eta^{(\prime)}$

$$
\begin{aligned}
M &= \frac{G_F}{\sqrt{2}}\Big\{V_{ub}V_{us}^* a_2 - V_{cb}V_{cs}^* a_2 \Delta i_5\big(\frac{m^2_{\eta^{(\prime)}}}{m_c^2}\big) \\
&- V_{tb}V_{ts}^*\Big[2(a_3-a_5)+\frac{1}{2}(a_9-a_7)+\Big(a_3-a_5-\frac{1}{2}(a_9-a_7)+a_4-\frac{1}{2}a_{10} \\
&\quad -(a_6-\frac{1}{2}a_8)\frac{m^2_{\eta^{(\prime)}}}{m_s(m_b+m_s)}\Big)\frac{f^s_{\eta^{(\prime)}}}{f^u_{\eta^{(\prime)}}} + (a_6-\frac{1}{2}a_8)\frac{m^2_{\eta^{(\prime)}}}{m_s(m_b+m_s)} \\
&+ (a_4-\frac{1}{2}a_{10})\frac{F_1^{B\to\eta^{(\prime)}}(m^2_{K^*})}{A_0^{B\to K^*}(m^2_{\eta^{(\prime)}})}\frac{f_{K^*}}{f^u_{\eta^{(\prime)}}}\Big]\Big\}\langle\overline{K^{0*}}|\overline{s}b_-|\overline{B^0}\rangle\langle\eta^{(\prime)}|\overline{u}u_-|0\rangle. \qquad (27)
\end{aligned}
$$

It is instructive to compare the matrix elements derived above with the corresponding expressions in [6], obtained by estimating the intrinsic charm quark content in the η, η' mesons. Concentrating on the decays $B^\pm \to (\eta',\eta)(K^\pm, K^{*\pm})$, which were the ones worked out in [6], and substituting

$$
\begin{aligned}
-\Delta i_5(m^2_{\eta'}/m_c^2)f^u_{\eta'} &\to f^c_{\eta'}, \\
-\Delta i_5(m^2_{\eta}/m_c^2)f^u_{\eta} &\to f^c_{\eta}, \qquad (28)
\end{aligned}
$$

we get (apart from the small electroweak penguin contributions neglected in [6] but included above) exactly the same expressions for the decay amplitudes as in [6]. Therefore, we have a simple relation between the decay constants $f^c_{\eta'}$, f^c_η, introduced in the intrinsic charm content method, and the form factor Δi_5 entering via the operator in Eq. (11). The idea of intrinsic charm quark content of η' and η and the contribution of the operator in Eq. (11) are related since this operator comes from the charm quark loop. Using the best-fit values of the (η,η')-mixing parameters from [24], yielding $\theta_8 = -22.2°, \theta_0 = -9.1°, f_8 = 168$ MeV, $f_0 = 157$ MeV, which in turn yields $f^u_{\eta'} = 63.6$ MeV and $f^u_\eta = 77.8$ MeV, the relations in (28) give $f^c_{\eta'} \sim -3.1$ MeV (-2.3 MeV) and $f^c_\eta \sim -1.2$ MeV (-0.9 MeV), with m_c having the value 1.3 GeV (1.5 GeV). The QCD-anomaly method gives results for f^c_η which are in good agreement with the ones in

[6] (in particular for $m_c = 1.5$ GeV) but it yields typically a factor 2 smaller value for $f^c_{\eta'}$ than the method based on the (η_c, η', η)-mixing [6]. Given the uncertainties in the fit parameters and approximations in both the methods, our estimates presented here are consistent with the parameters $f^c_{\eta'}$ and f^c_η obtained in [6].

However note that the two approaches are quite different. The advantage of the present approach is that the operator in Eq. (11) gives an unambiguous sign relative to the other contributions while the method of determining the intrinsic charm quark content via radiative decays $J/\psi \to (\eta_c, \eta', \eta)\gamma$ can only give the absolute magnitude. In our approach the relative signs of the contributions from O^c_1 and O^c_2 to the other contributions are determined; we obtain the negative-$f^c_{\eta'}$ (and f^c_η) solution of the two possible ones which were not resolved in [6].

4. Numerical results

For the numerical analysis, we take the values of the parameters used in [6]. The matrix elements listed in (**i**),...,(**iv**) depend on the effective coefficients $a_1, ..., a_{10}$, quark masses, various form factors, coupling constants and the CKM parameters. In turn, the coefficients a_i and the quark masses depend on the renormalization scale μ and the QCD scale parameter $\Lambda_{\overline{\rm MS}}$. We have fixed $\Lambda_{\overline{\rm MS}}$ using $\alpha_s(m_Z) = 0.118$, which is the central value of the present world average $\alpha_s(m_Z) = 0.118 \pm 0.003$ [30]. The scale μ is varied between $\mu = m_b$ and $\mu = m_b/2$, but due to the inclusion of the NLL expressions, the dependence of the decay rates on μ is small and hence not pursued any further. To be definite, we use $\mu = 2.5$ GeV in the following.. The CKM matrix will be expressed in terms of the Wolfenstein parameters [31], A, λ, ρ and η. Since the first two are well-determined with $A = 0.81 \pm 0.06$, $\lambda = \sin\theta_C = 0.2205 \pm 0.0018$, we fix them to their central values. The other two are correlated and are found to lie (at 95% C.L.) in the range $0.25 \le \eta \le 0.52$ and $-0.25 \le \rho \le 0.35$ from the CKM unitarity fits [32]. However, a good part of the negative-ρ region is now disfavoured [33] by the lower bound on the mass mixing ratio $\Delta M_s/\Delta M_d$ [34]. Likewise, the ratio $R_1 = 0.65 \pm 0.40$ measured recently by the CLEO collaboration [2], with $R_1 \equiv \mathcal{B}(B^0(\bar{B}^0) \to \pi^\pm K^\mp)/\mathcal{B}(B^\pm \to \pi^\pm K^0)$, disfavours the region $\rho < 0$ [6]. Hence, we shall not entertain here the negative-ρ values and take three representative points in the allowed (ρ, η) contour with $\rho \ge 0$. These correspond to the three values of the CKM matrix element ratio: $|V_{ub}/V_{cb}| = 0.08,\ 0.11,$ and 0.05, reflecting the present central value of this quantity and the upper and lower values resulting from a generous error on it. The specific values of ρ and η and the legends used in drawing the figures are as follows:

1. $\rho = 0.05, \eta = 0.36$, yielding $\sqrt{\rho^2 + \eta^2} = 0.36$ (drawn as a solid curve)
2. $\rho = 0.30, \eta = 0.42$, yielding $\sqrt{\rho^2 + \eta^2} = 0.51$ (drawn as a dashed curve)
3. $\rho = 0, \eta = 0.22$, yielding $\sqrt{\rho^2 + \eta^2} = 0.22$ (drawn as a dashed-dotted curve).

All other curves in Figs. 2 - 4, through which other parametric dependences are shown, are based on using the values $\rho = 0.05,\ \eta = 0.36$. The decay constants $f^u_{\eta'}$, $f^s_{\eta'}$, f^u_η and f^s_η can be obtained from f_0 and f_8 by using θ_0 and θ_8 for the η'-η mixing angles. Since $q^2 = m_h^2$ is rather close to the point $q^2 = 0$, and a simple pole model is mostly used to implement the q^2 dependence in the form factors, we shall neglect the q^2 dependence and equate $F^{B\to h}_{0,1}(q^2 = m_h^2) = F^{B\to h}_{0,1}(q^2 = 0)$. The values used for the form factors are listed in Table 1.

The quark masses enter our analysis in two different ways. First, they occur in the amplitudes involving penguin loops. We treat the internal quark masses in these loops as constituent

$F_{0,1}^{B\to K}$	$F_{0,1}^{B\to\eta'}$	$F_{0,1}^{B\to\eta}$	$A_0^{B\to K^*}$
0.33	$0.33\left[\frac{\sin\theta_8}{\sqrt{6}}+\frac{\cos\theta_0}{\sqrt{3}}\right]$	$0.33\left[\frac{\cos\theta_8}{\sqrt{6}}-\frac{\sin\theta_0}{\sqrt{3}}\right]$	0.28

Table 1: Form factors at $q^2 = 0$.

masses rather than current masses. For them we use the following (renormalization scale independent) values:

$$m_b = 4.88 \text{ GeV}, \quad m_c = 1.5 \text{ GeV}, \quad m_s = 0.5 \text{ GeV}, \; m_d = m_u = 0.2 \text{ GeV}. \tag{29}$$

Variation in a reasonable range of these parameters does not change the numerical results of the branching ratios significantly. The value of m_b above is fixed to be the current quark mass value $\overline{m_b}(\mu = m_b/2) = 4.88$ GeV, given below. Second, the quark masses m_b, m_s, m_d and m_u also appear through the equations of motion when working out the (factorized) hadronic matrix elements. In this case, the quark masses should be interpreted as current masses. Using $\overline{m_b}(m_b) = 4.45$ GeV [35] and

$$\overline{m_s}(1 \text{ GeV}) = 150 \text{ MeV} \quad , \quad \overline{m_d}(1 \text{ GeV}) = 9.3 \text{ MeV} \quad , \quad \overline{m_u}(1 \text{ GeV}) = 5.1 \text{ MeV} \quad , \tag{30}$$

from [36], the corresponding values at the renormalization scale $\mu = 2.5$ GeV are given in Table 2, together with other input parameters needed for our analysis.

$\overline{m_b}$	$\overline{m_s}$	$\overline{m_d}$	$\overline{m_u}$	$\alpha_s(m_Z)$	τ_B
4.88 GeV	122 MeV	7.6 MeV	4.2 MeV	0.118	1.60 ps

Table 2: Quark masses and other input parameters. The running masses are given at the renormalization scale $\mu = 2.5$ GeV in the $\overline{\text{MS}}$ scheme.

The branching ratios $BR(B^\pm \to \eta' K^\pm)$ and $BR(B^0 \to \eta' K^0)$ are plotted against the parameter ξ in Figs. 2 and 3, respectively. Although not indicated by the notation, the branching ratios for the neutral B-meson decays are always understood to be averages with the corresponding charged conjugated decays in the following tables and figures. We would like to make the following observations concerning the sensitivity of the branching ratios on the various input parameters.

- CKM-parametric dependence: The branching ratio $BR(B^\pm \to \eta' K^\pm)$ shows a mild dependence (of order 10%) on the CKM parameters whereas $BR(B^0 \to \eta' K^0)$ is practically independent of them.

- s-quark mass dependence: The dependence of the branching ratios on the s-quark mass is quite marked. To illustrate this we show the two branching ratios calculated using $\overline{m_s}(2.5 \text{ GeV}) = 100$ MeV through the dotted curves, to be compared with the corresponding solid curves which are drawn for the same values of the CKM parameters, namely $\rho = 0.05$ and $\eta = 0.36$, but $\overline{m_s}(2.5 \text{ GeV}) = 122$ MeV. The resulting increase in

Processes	BR ($\xi = 0$)	BR ($\xi = 0.45$)	Experiment
$B^\pm \to \eta' K^\pm$	$(2.7 - 3.6) \times 10^{-5}$	$(2.0 - 2.6) \times 10^{-5}$	$(6.5^{+1.5}_{-1.4} \pm 0.9) \times 10^{-5}$
$B^\pm \to \eta' K^{*\pm}$	$(2.6 - 5.2) \times 10^{-7}$	$(2.0 - 3.9) \times 10^{-7}$	$< 1.3 \times 10^{-4}$
$B^\pm \to \eta K^\pm$	$(1.5 - 2.2) \times 10^{-6}$	$(0.8 - 1.7) \times 10^{-6}$	$< 1.4 \times 10^{-5}$
$B^\pm \to \eta K^{*\pm}$	$(1.5 - 3.0) \times 10^{-6}$	$(1.6 - 3.1) \times 10^{-6}$	$< 3.0 \times 10^{-5}$
$B^0 \to \eta' K^0$	$(3.0 - 3.7) \times 10^{-5}$	$(2.0 - 2.6) \times 10^{-5}$	$(4.7^{+2.7}_{-2.0} \pm 0.9) \times 10^{-5}$
$B^0 \to \eta' K^{*0}$	$(2.0 - 6.5) \times 10^{-7}$	$(0.8 - 1.0) \times 10^{-7}$	$< 3.9 \times 10^{-5}$
$B^0 \to \eta K^0$	$(1.2 - 1.7) \times 10^{-6}$	$(0.8 - 1.1) \times 10^{-6}$	$< 3.3 \times 10^{-5}$
$B^0 \to \eta K^{*0}$	$(2.4 - 3.4) \times 10^{-6}$	$(1.9 - 2.8) \times 10^{-6}$	$< 3.0 \times 10^{-5}$

Table 3: Numerical estimates of the branching ratios for the decays $B^\pm \to (\eta', \eta)(K^\pm, K^{*\pm})$ and $B^0 \to (\eta', \eta)(K^0, K^{*0})$, obtained by varying the CKM parameters in the ranges indicated in the text and the s-quark mass in the range 100 MeV $\leq \overline{m_s}(2.5\ \text{GeV}) \leq$ 122 MeV. The first column corresponds to using the value of the factorization-model parameter $\xi = 0$ and the second to $\xi = 0.45$. The third column shows the present measurement and the 90% C.L. upper limits reported by the CLEO collaboration [1, 5].

the branching ratios in lowering the value from $\overline{m_s} = 122$ MeV to $\overline{m_s} = 100$ MeV amounts to about 20% (and 65% for $\overline{m_s} = 80$ MeV). While in literature one comes across even smaller values of $\overline{m_s}(2.5\ \text{GeV})$, we subscribe to the view that the value $\overline{m_s}(2.5\ \text{GeV}) = 100$ MeV is a realistic lower limit on this quantity. However, if the present high values of the branching ratios for $B^\pm \to \eta' K^\pm$ and $B^0 \to \eta' K^0$ continue to persist, one might have to consider smaller values of $\overline{m_s}$. We also expect progress in calculating quark masses on the lattice, sharpening the theoretical estimates presented here.

- Dependence on $f^c_{\eta'}$: Restricting to the negative-$f^c_{\eta'}$ solution, determined by the QCD-anomaly method, we plot the branching ratios with $f^c_{\eta'} = -5.8$ MeV, as obtained in [6]. The other parameters are: $\overline{m_s}(2.5\ \text{GeV}) = 100$ MeV, $\rho = 0.05$ and η=0.35. The results are shown through the long-short dashed curves in Figs. 2 and 3. Comparing these curves with the corresponding dotted curves, we see that the resulting branching ratios in the two approaches are very similar.

- Dependence on ξ: This amounts to between 20% and 35% depending on the other parameters if one varies ξ in the range $0 \leq \xi \leq 0.5$. In all cases, the branching ratios are larger for $\xi = 0$.

Taking into account the parametric dependences just discussed, we note that the theoretical branching ratios $BR(B^\pm \to \eta' K^\pm)$ and $BR(B^0 \to \eta' K^0)$ are uncertain by a factor 2. Determining the value of ξ from other $B \to h_1 h_2$ decays in the future, this uncertainty can be reduced considerably (see Table 3).

The ratio of the branching ratios $BR(B^\pm \to \eta' K^\pm)/BR(B^0 \to \eta' K^0)$ is a useful quantity, as it is practically independent of the form factors and most input parameters. This is shown in Fig. 4. We see that the residual uncertainty is due to the CKM-parameter dependence of

this ratio, which is estimated as about 10%. We get (for $0 \leq \xi \leq 0.5$)

$$\frac{BR(B^\pm \to \eta' K^\pm)}{BR(B^0 \to \eta' K^0)} = 0.9 - 1.02 \ . \tag{31}$$

The present experimental value of this ratio as calculated by adding the experimental errors in the numerator and denominator in quadrature is 1.38 ± 0.86. Given the large experimental error, it is difficult to draw any quantitative conclusions except that the theoretical ratio in Eq. (31) is in agreement with data. However, we do expect that the experimental value of this ratio will asymptote to unity.

The branching ratio $BR(B^\pm \to \eta' K^\pm)$ is found to be somewhat lower than the present experimental number reported by CLEO. As shown in Fig. 2, we estimate $BR(B^\pm \to \eta' K^\pm) = (2-4) \times 10^{-5}$ in our framework compared to the experimental measurement of the same $(6.5 \pm 1.75) \times 10^{-5}$. The calculations presented here are in better agreement with the experimental measurement of $BR(B^0 \to \eta' K^0)$, making it to within 1σ. Of course, theoretical rates can be augmented by increasing the values of the input form factors given in Table 1. There is certainly some room for such enhancement, but in view of the emerging theoretical consensus on the estimates of the form factors and the fact that the branching ratios in a number of $B \to h_1 h_2$ decays do not require such enhancement [6], this can only be modest. Hence, we anticipate that the experimental numbers for $BR(B^\pm \to \eta' K^\pm)$ and $BR(B^0 \to \eta' K^0)$ will decrease so as to be more in line with the rest of the CKM-allowed QCD-penguin-dominated two-body B decays and with our estimates!

We present in Table 3 numerical estimates for all the eight branching ratios $BR(B^\pm \to (\eta', \eta)(K^\pm, K^{*\pm}))$ and $BR(B^0 \to (\eta', \eta)(K^0, K^{*0}))$ calculated in the QCD-anomaly method. The ranges shown take into account the m_s- and CKM-parametric dependence, discussed earlier. The entries in column 2 and 3 are based on the choice $\xi = 0$, corresponding to using $N_c = \infty$ in the effective coefficients, and $\xi = 0.45$, which corresponds to the phenomenological value estimated in the decays $B \to (D, D^*)(\pi, \rho)$ [20], respectively

A number of comments are in order on the entries in Table 3. First, as shown in this table and Fig. 4, theoretical estimates of the branching ratios for $B^\pm \to \eta' K^\pm$ and $B^0 \to \eta' K^0$ are almost equal and they are also the largest for the eight decays shown. So, it is no coincidence that these are exactly the ones measured so far. In particular, the branching ratios for the decays $B^\pm \to \eta' K^{*\pm}$ and $B^0 \to \eta' K^{*0}$ are found to be the smallest in this group, and we predict

$$\frac{BR(B^\pm \to \eta' K^{*\pm})}{BR(B^\pm \to \eta' K^\pm)} \leq 0.02 \ , \tag{32}$$

$$\frac{BR(B^0 \to \eta' K^{*0})}{BR(B^0 \to \eta' K^0)} \leq 0.03 \ . \tag{33}$$

Likewise, the branching ratios for the decay modes $B^\pm \to \eta K^\pm$ and $B^0 \to \eta K^0$ are smaller compared to their η'-counterparts by at least an order of magnitude. We estimate $BR(B^\pm \to \eta K^\pm) = (1-2) \times 10^{-6}$ and a similar value for the neutral B decay mode. On the other hand, the branching ratios for the decay modes $B^\pm \to \eta(K^\pm, K^{*\pm})$ and $B^0 \to \eta(K^0, K^{*0})$ are all comparable to each other and are predicted to be somewhere in the range $(1-3) \times 10^{-6}$. The reason behind this pattern can be seen in the various constructive and destructive

interferences involving the eight amplitudes listed earlier. This is in qualitative agreement with the anticipation in [37].

5. Concluding Remarks

We have provided an independent estimate of the process $b \to s(c\bar{c}) \to s(gg) \to s(\eta', \eta)$, using QCD anomaly. The resulting branching ratios in $B \to (\eta', \eta)(K, K^*)$ reported here are close to the ones obtained in the (η_c, η', η)-mixing approach [6]. The present method also removes the intrinsic sign ambiguity inherent in ref. [6], thereby reducing one source of calculational uncertainty. Theoretical predictivity is, however, still limited due to the remaining input parameters of this framework and we estimate it to be a factor 2. Despite this, very clear patterns emerge among the various decay modes considered here, which are drastically different from the ones which follow in other scenarios. Hence, ongoing and future experiments will be able to test the predictions of the present approach as well as of the competing ones, such as models based on the dominance of the intrinsic charm contributions in η', as suggested in [8, 9], or models in which dominant role is attributed to the soft-gluon-fusion process to form an η or η' [17, 18]. In contrast to our approach, these models typically predict similar branching ratios (within a factor 2) involving the modes $B \to \eta' K$ and $B \to \eta' K^*$, in both the charged and neutral B decays. Data already rules out models predicting $BR(B \to \eta' K^*) > BR(B \to \eta' K)$, and is tantalizingly close to testing also the soft-gluon fusion models which predict $BR(B \to \eta' K^*) \simeq 0.5 BR(B \to \eta' K)$ [17, 18]. We note that a large intrinsic-charm component in η' is not substantiated by independent analysis of the $\eta'\gamma$ form factor [24]. Soft-gluon-fusion models are not theoretically motivated as they show extreme (quartic) sensitivity of the decay widths to the gluon mass (an ill-defined quantity) – reflecting that the method being employed in these models is neither infrared stable nor predictive. For a definite test of the theoretical framework presented here and in [6], more precise data are required and one has to reduce the uncertainty on the input parameters, in particular the s-quark mass. However, if in forthcoming experiments, the branching ratios presented in Table 3 for the eight decay modes are found to be significantly larger (in particular in the modes $B^{\pm} \to \eta' K^{*\pm}$ and $B^0 \to \eta' K^{*0}$), then it will most probably be an indication of significant non-factorizing contributions, which may feed into the decays $B \to (\eta', \eta)(K, K^*)$ dominantly through the matrix elements of the dipole operator O_g.

In conclusion, we reiterate the two intrinsic assumptions of our approach: (i) absence of final state interactions, and (ii) absence of non-perturbative contributions in penguin diagrams, which may modify both the magnitudes and phases of the effective coefficients calculated in the factorization framework presented here. The first should be a good approximation for the decays being considered. For the second, we note that non-perturbative contributions are not specific to the decays $B \to (\eta', \eta)(K, K^*)$ but are endemic to all such decays where penguins play a dominant role [38]. Furthermore, we admit that the factorization framework used here and elsewhere is vulnerable and it is conceivable that non-perturbative non-factorizing contributions do play a significant role in non-leptonic two-body B-decays being discussed here. This remains to be tested experimentally or proven on firm theoretical grounds in a well-defined framework, such as lattice QCD. However, it is fair to say that there exists at least a *prima facie* case in some of the related decays, such as $B \to K\pi$ and $B \to \pi\pi$, which support the contention that the neglected non-perturbative effects are not overwhelming and the measured decay rates can be explained without invoking them [6]. Of course, this point of view may have to be revised with more precise data.

Acknowledgment

JC and PK are grateful to DESY for hospitality, where this work was initiated. AA would like to thank Professor H.S. Song for the hospitality at Seoul National University. This work has been partially supported by the German-Korean scientific exchange programme DFG-446-KOR-113/72/0 and by Schweizerischer Nationalfonds. JC and PK were supported in part by the Ministry of Education grants BSRI 97-2408 and BSRI 97-2418, respectively, and the Korea Science and Engineering Foundation (KOSEF) through the SRC program of SNU-CTP, and the Distinguished Scholar Exchange Program of Korea Research Foundation. PK is also supported in part by KOSEF, Contract 971-0201-002-2. We would like to thank Thorsten Feldmann, Gustav Kramer, Heiri Leutwyler, Peter Minkowski, Hubert Simma and Jim Smith for discussions.

References

[1] J. Smith (CLEO Collaboration), talk presented at the 1997 ASPEN winter conference on Particle Physics, Aspen, Colorado, 1997 ; S. Anderson et al. (CLEO Collaboration), CLEO CONF 97-22a and EPS 97-333 (1997).

[2] R. Godang et al. (CLEO Collaboration), preprint CLNS 97-1522, CLEO 97-27 (1997).

[3] M.S. Alam et al. (CLEO Collaboration), CLEO CONF 97-23 and EPS 97-335 (1997).

[4] J. Roy (CLEO Collaboration), invited talk at the Heavy Flavour Workshop, Rostock, September 1997.

[5] B.H. Behrens et al. (CLEO Collaboration), CLNS 97/1536, CLEO 97-31, hep-ex/9801012 (1998).

[6] A. Ali and C. Greub, hep-ph/9707251, Phys. Rev. D (in press).

[7] D. Atwood and A. Soni, Phys. Lett. **B405** (1997) 150 and hep-ph/9706512.

[8] I. Halperin and A. Zhitnitsky, Phys. Rev. **D56** (1997) 7247; hep-ph/9705251.

[9] E. Shuryak and A.R. Zhitnitsky, hep-ph/9706316.

[10] W.S. Hou and B. Tseng, Phys. Rev. Lett. **80** (1998) 434.

[11] F. Yuan and K.T. Chao, Phys. Rev. **D56** (1997) 2495.

[12] A. Datta, X.-G. He and S. Pakvasa, UH-511-864-97, ISU-HET-97-07, hep-ph/9707259.

[13] H.-Y. Cheng and B. Tseng, Phys. Lett. **B415** (1997) 263.

[14] A. Kagan and A.A. Petrov , UCHEP-27, UMHEP-443, hep-ph/9707354.

[15] A.S. Dighe, M. Gronau and J. Rosner, Phys. Rev. Lett. **79** (1997) 4333.

[16] N.G. Deshpande, B. Dutta and S. Oh, OITS-641, COLO-HEP-389, hep-ph/9710354.

[17] M.R. Ahmady, E. Kou and A. Sugomoto, preprint hep-ph/9710509.

[18] D. Du, C.S. Kim and Y. Yang, preprint hep-ph/9711428.

[19] M. Bauer and B. Stech, Phys. Lett. **B152** (1985) 380;
M. Bauer, B. Stech and M. Wirbel, Z. Phys. **C34** (1987) 103.

[20] M. Neubert and B. Stech, preprint CERN-TH/97-99 [hep-ph 9705292], to appear in *Heavy Flavors*, Second Edition, ed. A.J. Buras and M. Lindner (World Scientific, Singapore).

[21] K. Berkelman (unpublished CLEO note).

[22] F.J. Gilman and R. Kaufman, Phys. Rev. **D36** (1987) 2761. See also, *Dynamics of the Standard Model.* authors: J.F. Donoghue. E. Golowich and B. Holstein, Cambridge University Press, 1992.

[23] H. Leutwyler, preprint hep-ph/9709408;
P. Herrera-Sikoldy, J.I. Latorre, P. Pascual and J. Taron, preprint hep-ph/9710268.

[24] T. Feldmann and P. Kroll, preprint WUB 97-28, hep-ph/9711231.

[25] A. Ali, G. Kramer and C.-D. Lü (to be published).

[26] A.J. Buras et al., Nucl. Phys. **B370** (1992) 69;
M. Ciuchini, E. Franco and L. Reina, Nucl. Phys. **B415** (1994) 403.

[27] H. Simma and D. Wyler, Nucl. Phys. **B344** (1990) 283.

[28] M.B. Voloshin, Phys. Lett. **B397** (1997) 275.

[29] M. Voloshin and V. Zakharov, Phys. Rev. Lett. **45** (1980) 688;
P. Ball, J.-M.. Frère and M. Tytgat, Phys. Lett. **B365** (1996) 367.

[30] M. Schmelling, preprint hep-ex/9701002.

[31] L. Wolfenstein, Phys. Rev. Lett. **51** (1983) 1945.

[32] A. Ali and D. London, Nucl. Phys. B (Proc. Suppl.) **54A** (1997) 297;
A. Ali, Acta Physica Polonica **B27** (1996) 3529.

[33] P. Paganini, F. Parodi, R. Roudeau and A. Stochi, hep-ph/9711261;
A. Ali, preprint DESY 97-256, hep-ph/9801270, to appear in Proc. of the First APCTP Workshop, Pacific Particle Physics Phenomenology, Seoul, South Korea, Oct. 31 - Nov. 2, 1997.

[34] M. Feindt, plenary talk, EPS Conference, Jerusalem 1997.

[35] M. Gremm, A. Kapustin, Z. Ligeti and M.B. Wise, Phys. Rev. Lett. **77** (1996) 20.

[36] J. Gasser and H. Leutwyler, Nucl. Phys. **B250** (1985) 465.

[37] H.J. Lipkin, Phys. Lett. **B254** (1991) 247.

[38] M. Ciuchini et al., Nucl. Phys. **B50** (1997) 271.

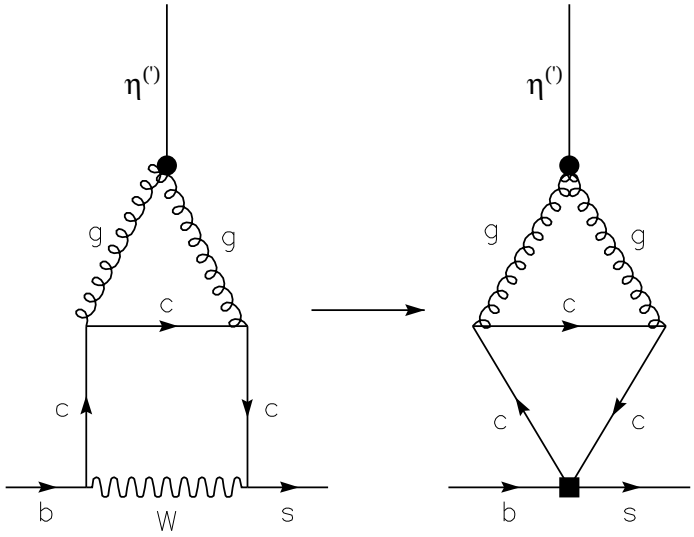

Figure 1: Feynman diagram contributing to the processes $b \to s(c\bar{c}) \to s(gg) \to s\eta^{(\prime)}$ in the full and effective theory. The lower vertex in the diagram on the right is calculated with the insertion of the operators O_1^c and O_2^c in the effective Hamiltonian approach; the upper vertex in both the full and effective theory is determined by the QCD triangle anomaly.

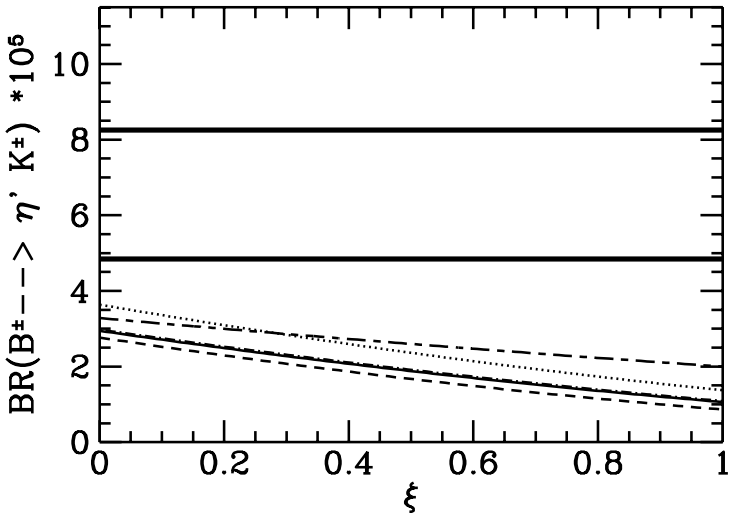

Figure 2: The branching ratio $BR(B^{\pm} \to \eta' K^{\pm})$ plotted against the parameter ξ. The lower three curves correspond to the value $\overline{m_s}(2.5\ \text{GeV}) = 122$ MeV and the three choices of the CKM parameters: $\rho = 0.05, \eta = 0.36$ (solid curve); $\rho = 0.30, \eta = 0.42$ (dashed curve); $\rho = 0, \eta = 0.22$ (dashed-dotted curve). The upper two curves correspond to the value $\overline{m_s}(2.5\ \text{GeV}) = 100$ MeV, $\rho = 0.05, \eta = 0.36$ and $f_{\eta'}^c = -2.3$ MeV from the QCD-anomaly method (dotted curve) and $f_{\eta'}^c = -5.8$ MeV from [6] (long-short dashed curve). The horizontal thick solid lines represent the present CLEO measurements (with $\pm 1\sigma$ errors).

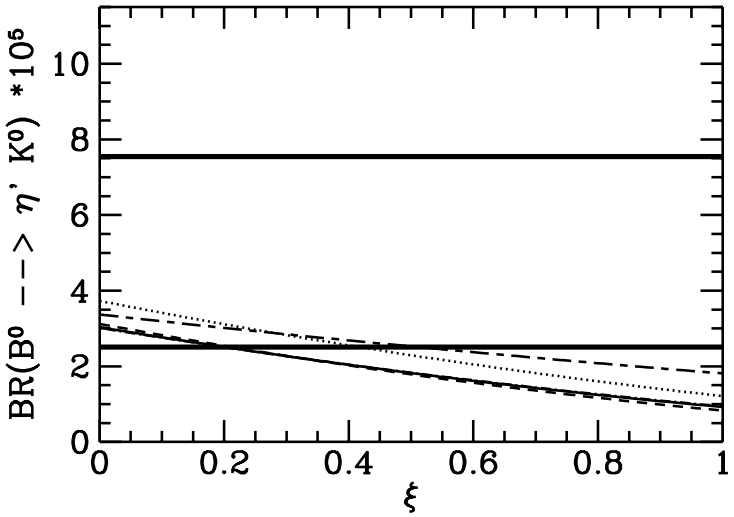

Figure 3: The branching ratio $BR(B^0 \to \eta' K^0)$ plotted against the parameter ξ. The legends are the same as in Fig. 2. The horizontal thick solid lines represent the present CLEO measurements (with $\pm 1\sigma$ errors).

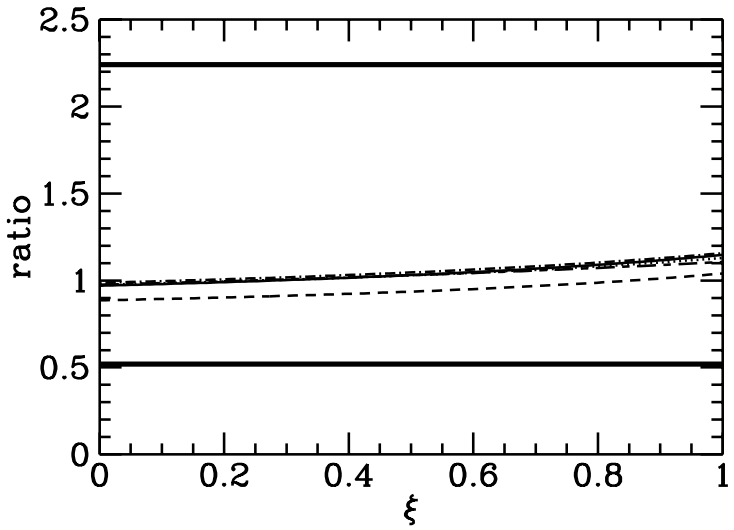

Figure 4: Ratio of the branching ratios $BR(B^\pm \to \eta' K^\pm)/\ BR(B^0 \to \eta' K^0)$ plotted against the parameter ξ. The legends are the same as in Fig. 2. The horizontal thick solid lines represent the present CLEO measurements (with $\pm 1\sigma$ errors estimated as stated in the text).